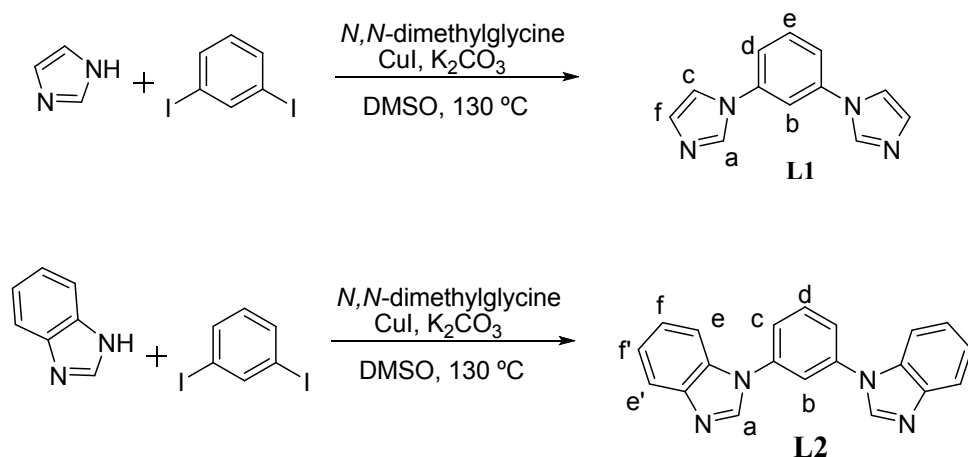


Nanoscale metallogel via self-assembly of self-assembled trinuclear coordination rings: Multi-stimuli-responsive soft materials

Sudhakar Ganta and Dillip Kumar Chand*

Supporting Information

Synthesis of ligands: The ligands **L1** and **L2** were synthesized by following reported literature procedures as mentioned in the manuscript (detail below).



Scheme S1. Synthesis of the ligands **L1** and **L2**.

1,3-bis(1-imidazolyl)benzene, L1: A mixture of CuI (228 mg, 1.2 mmol), *N,N*-dimethylglycine (350 mg, 2.4 mmol), K₂CO₃ (4.2 g, 30 mmol), imidazole (1.24 g, 18 mmol), and 1,3-diiodobenzene (2 g, 6 mmol) in 50 mL DMSO was heated at 130 °C for 48 h under N₂ atmosphere in a round bottom flask. Then the mixture was cooled down to room temperature and partitioned between water (50 mL) and ethyl acetate (100 mL). The organic layer was separated and the aqueous fraction was extracted with ethyl acetate twice (2 x 50 mL). The combined organic layer was washed with NaHCO₃, dried over Na₂SO₄ and concentrated in vacuum which leads to an off white powder of the ligand, **L1**. Yield: 0.882 g, 70% (based on 1,3-diiodobenzene).

1,3-bis(1-benzo[d]imidazolyl)benzene, L2 : A mixture of CuI (228 mg, 1.2 mmol), *N,N*-dimethylglycine (350 mg, 2.4 mmol), K₂CO₃ (4.2 g, 30 mmol), benzimidazole (2.15 g, 18 mmol), and 1,3-diiodobenzene (2 g, 6 mmol) in 50 mL DMSO was heated at 130 °C for 48 h under N₂ atmosphere. Then the mixture was cooled down to room temperature and partitioned between water (50 mL) and ethyl acetate (100 mL). The organic layer was separated and the aqueous fraction was extracted with ethyl acetate twice (2 x 50 mL). The combined organic layers were washed with NaHCO₃, dried over Na₂SO₄ and concentrated in vacuum which leads to yellow powder, which was further purified by column chromatography with acetone: CH₂Cl₂ in 2:1 ratio to get pale yellow powder of ligand, **L2**. Yield: 1.190 g, 64% (based on 1,3-diiodobenzene).

The residual solvent peaks in the NMR spectra recoded in DMSO-d₆ are calibrated using TMS as external standard.

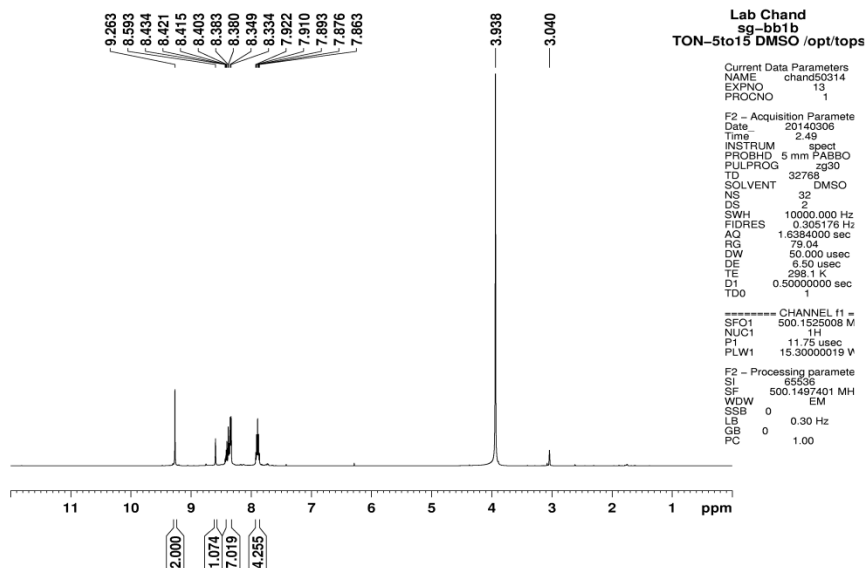


Fig S1. 500 MHz ¹H NMR spectrum of the ligand, **L2** in DMSO-d₆.

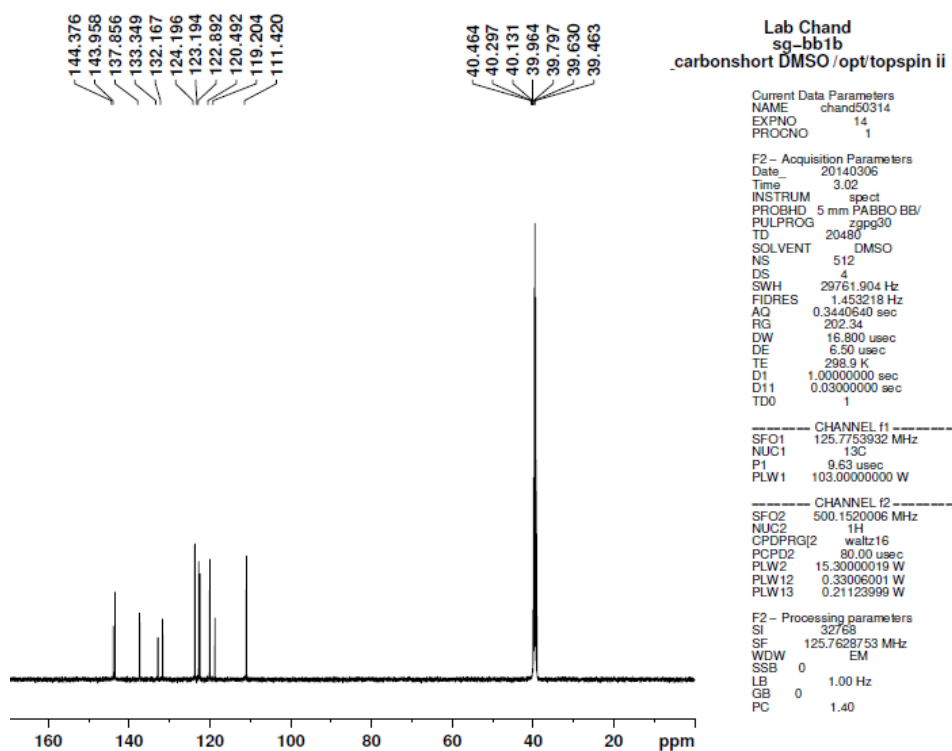


Fig S2. 125 MHz ¹³C NMR spectrum of the ligand, **L2** in DMSO-d₆.

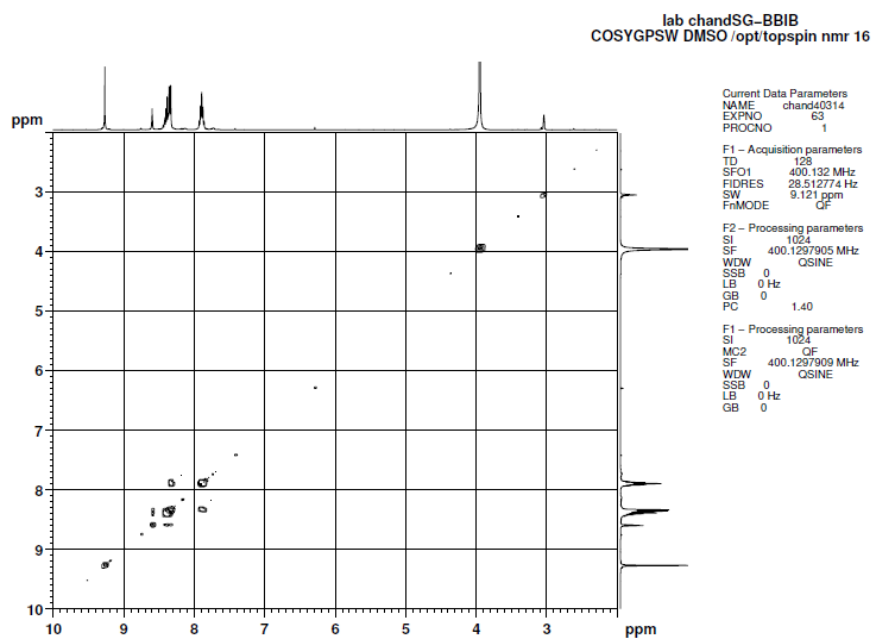


Fig S3. H-H COSY of the ligand, **L2** in DMSO- d_6 .

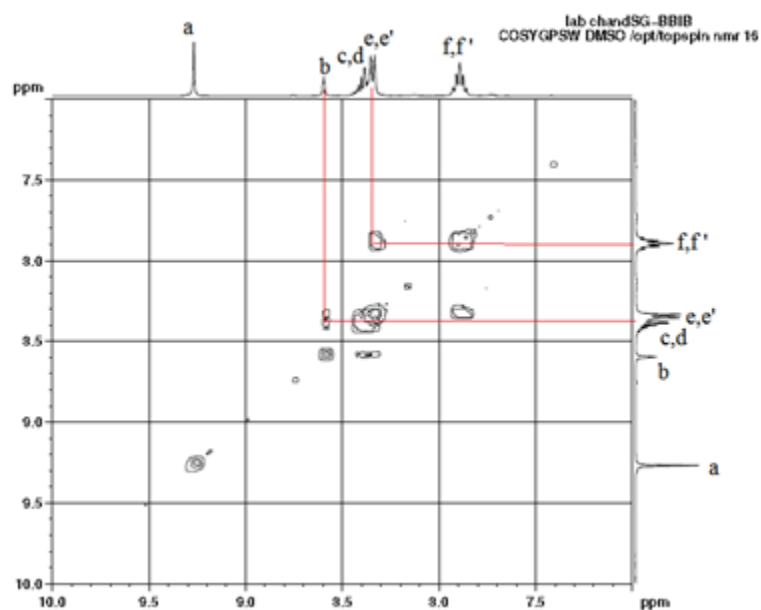


Fig S4. Expansion of H-H COSY of the ligand, **L2** in DMSO- d_6 .

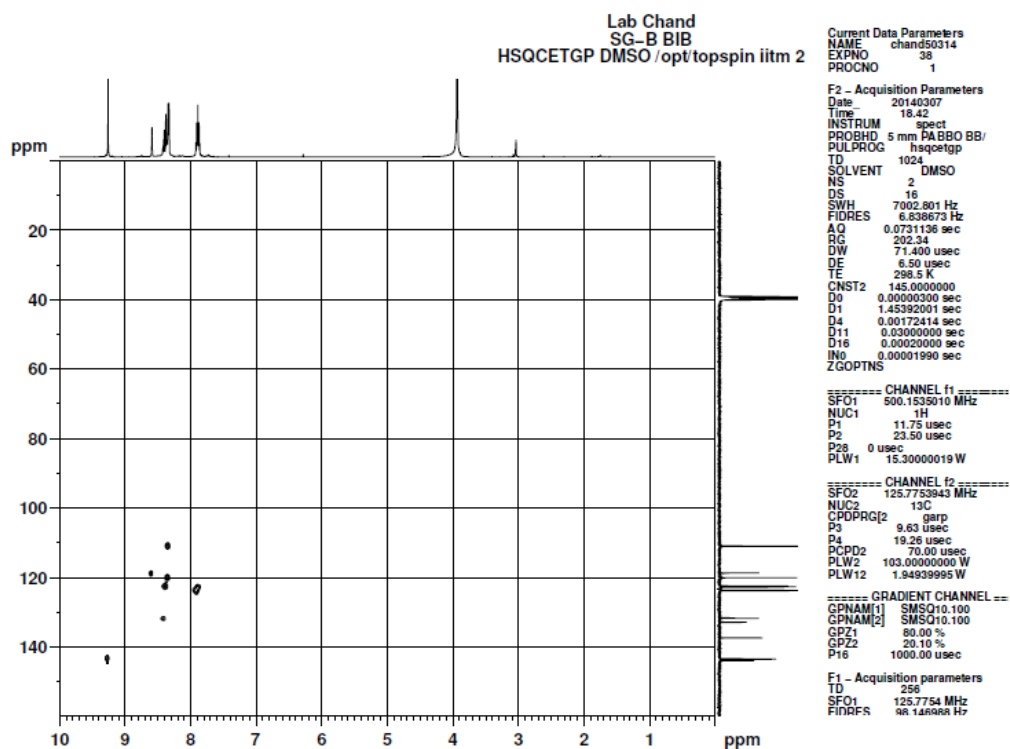


Fig S5: C-H COSY of the ligand, **L2** in DMSO- d_6 .

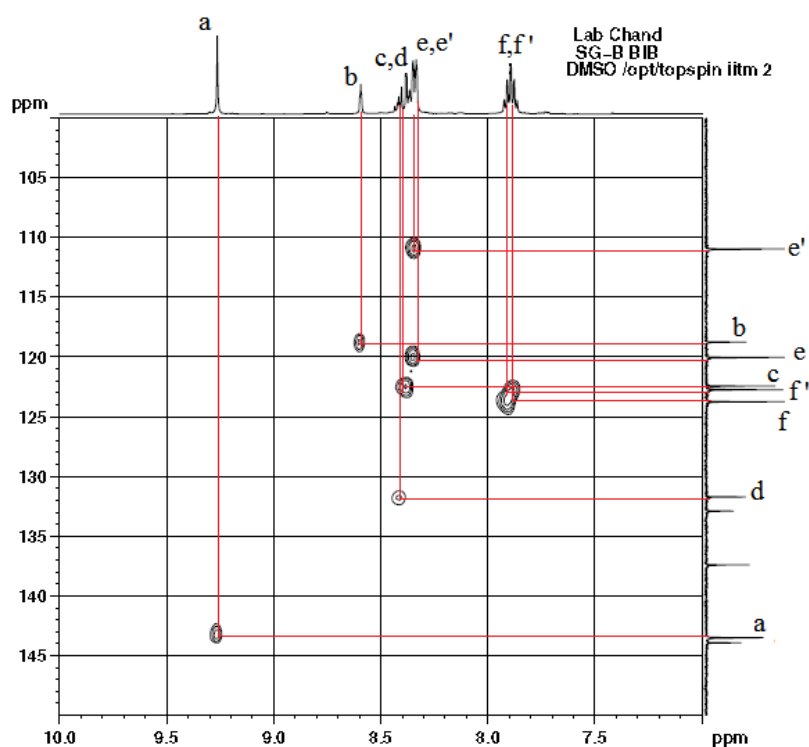
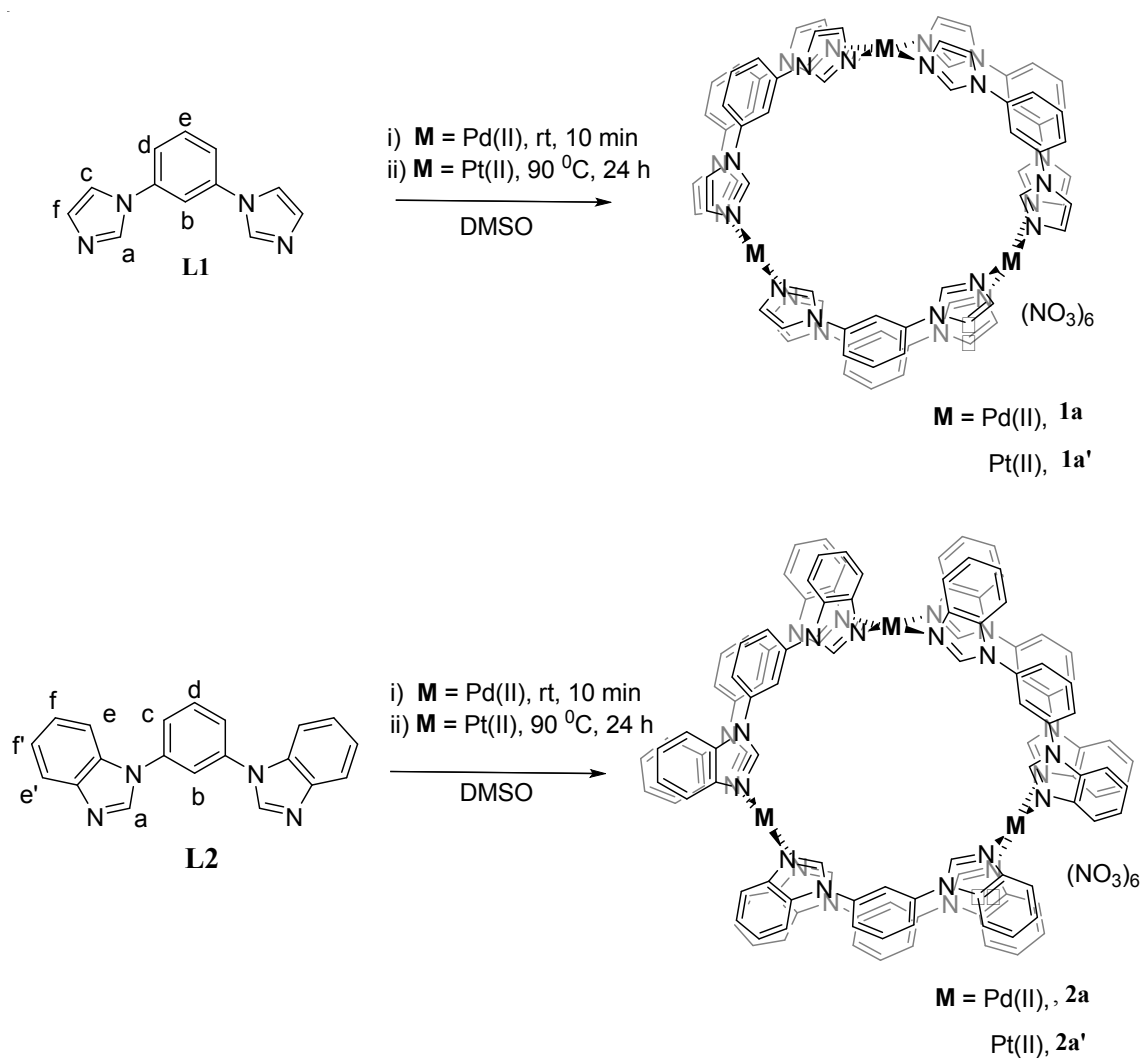


Fig S6: C-H COSY of the ligand, **L2** in DMSO- d_6 .



Scheme S2. Synthesis of the complexes **1a**, **1a'**, **2a** and **2a'**.

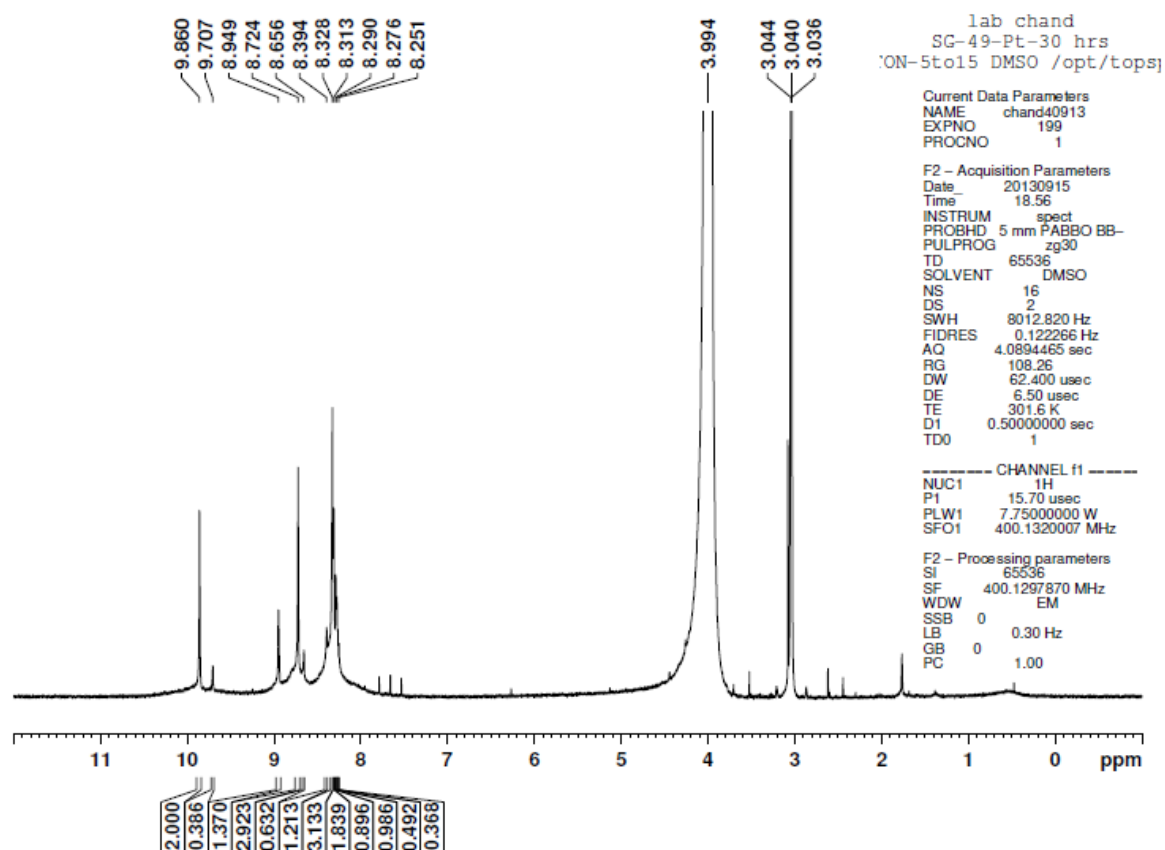


Fig S7: 400 MHz ^1H NMR spectrum of the complex **1a'** in DMSO- d_6 .

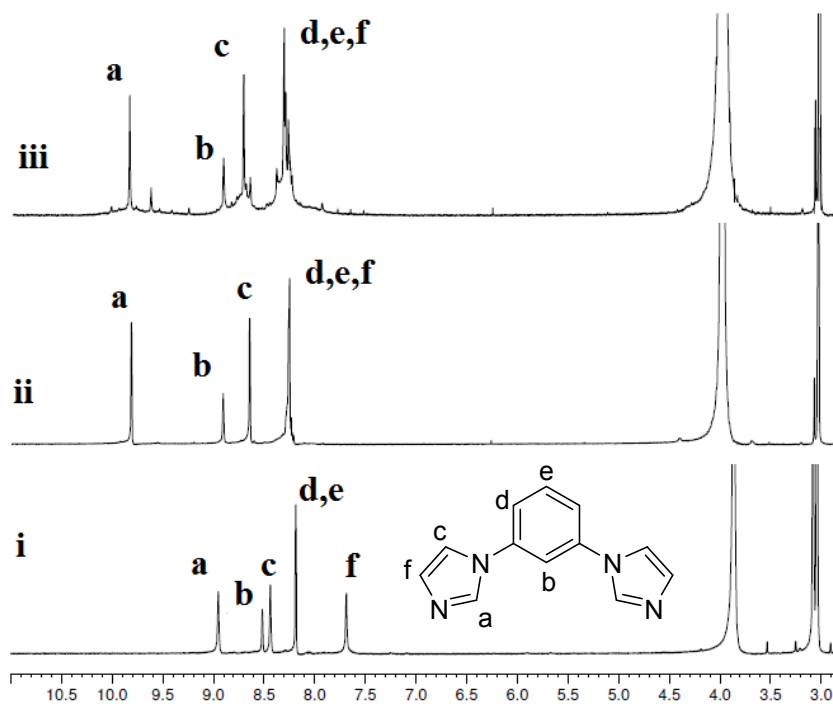


Figure S8: Comparison of ^1H NMR spectra of i) ligand **L1**, ii) $[\text{Pd}_3(\text{L1})_6](\text{NO}_3)_6$, **1a** and iii) $[\text{Pt}_3(\text{L1})_6](\text{NO}_3)_6$, **1a'** in DMSO- d_6 .

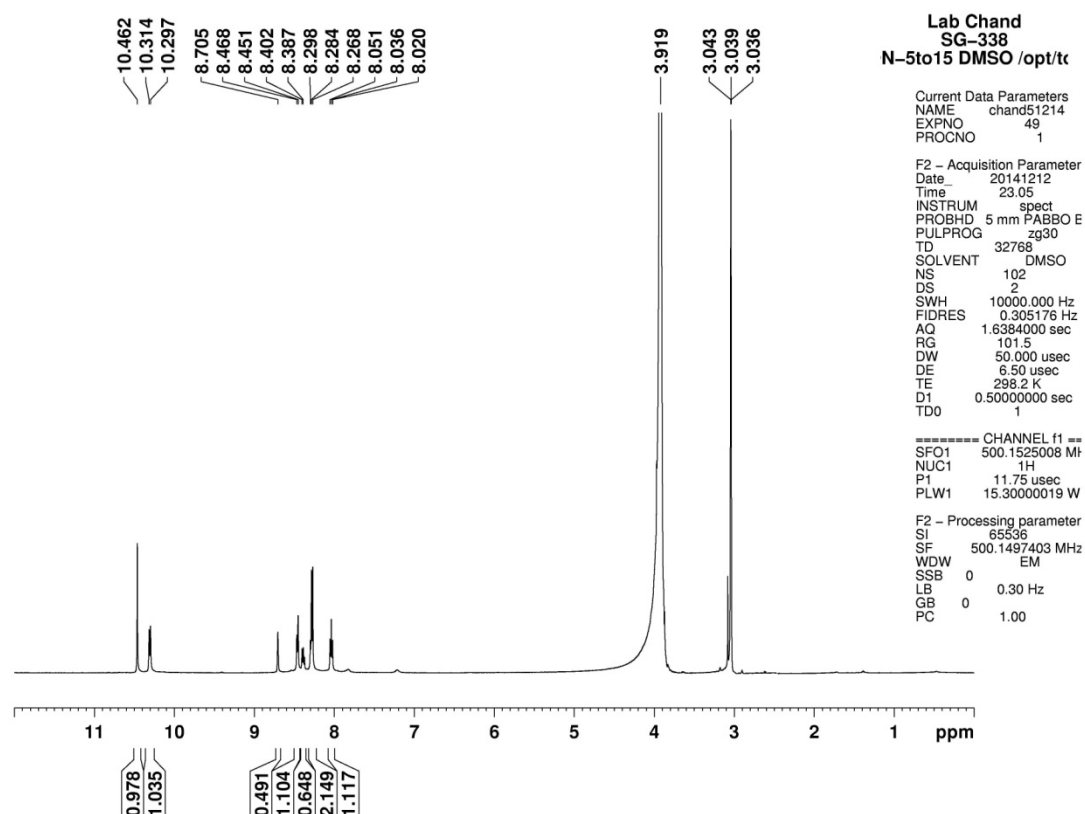


Fig S9: 500 MHz ^1H NMR spectrum of **2a** in DMSO- d_6 .

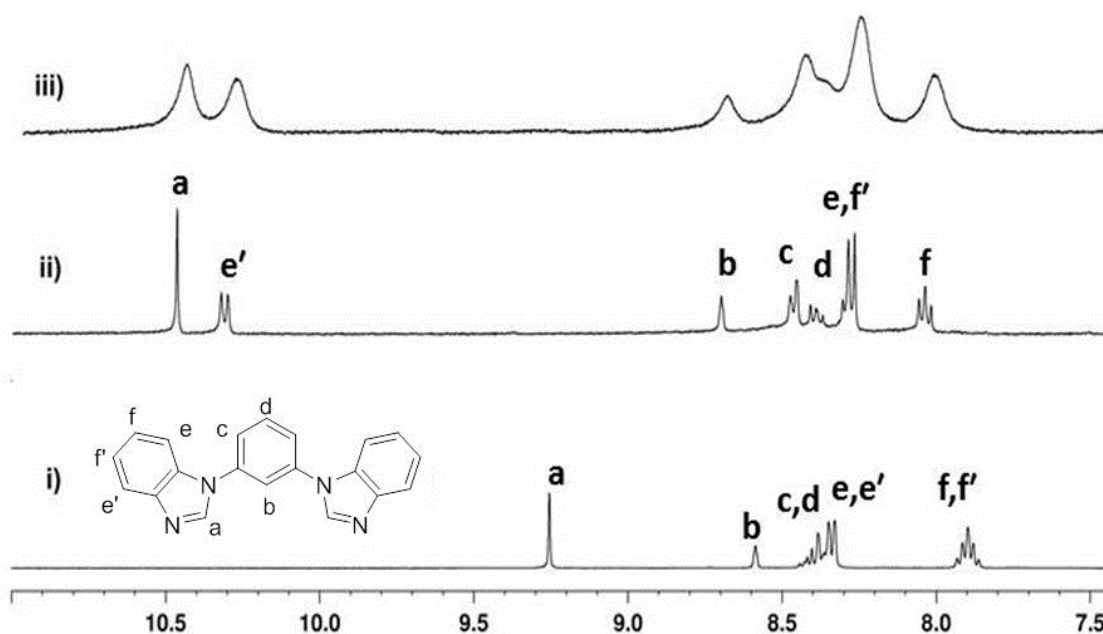


Fig S10: Comparison of ^1H NMR spectra of i) the ligand, **L2**, complex **2a** ii) 2 mM and iii) 6 mM concentration in DMSO- d_6 .

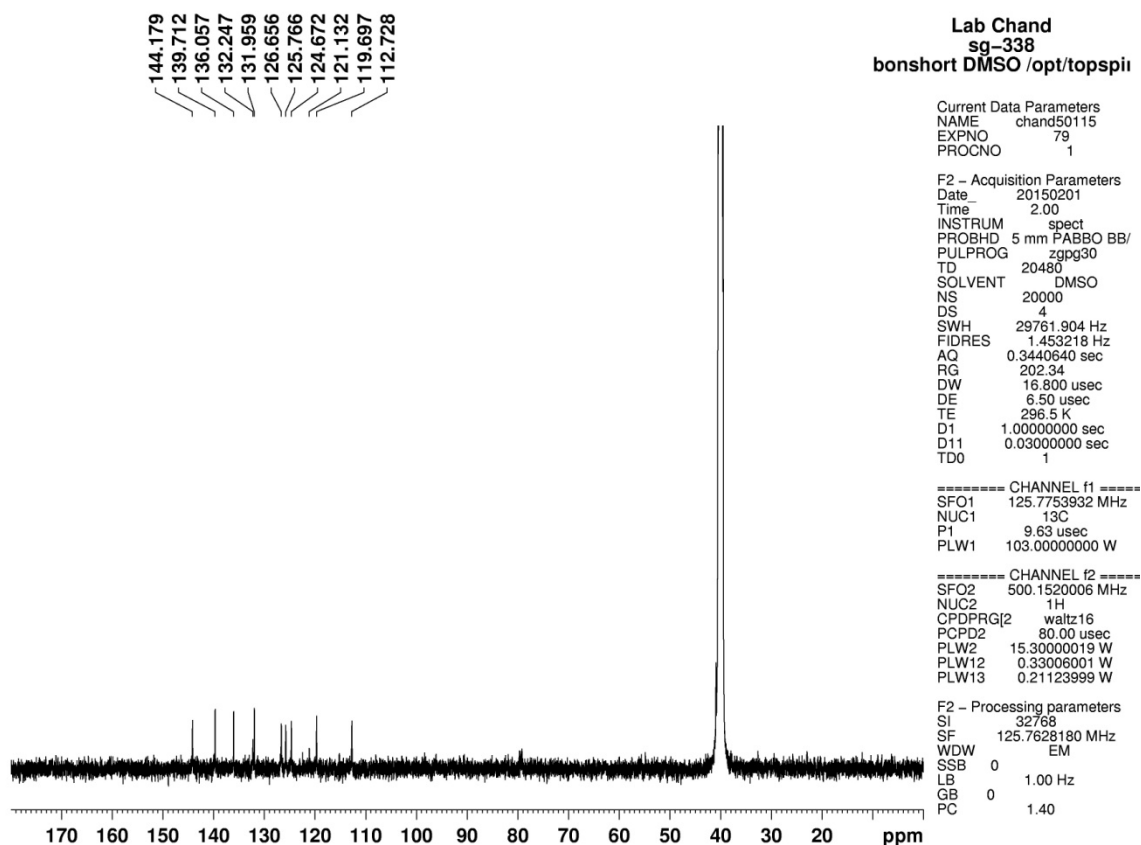


Fig S11: 125 MHz ^{13}C NMR spectrum of **2a** in DMSO- d_6 .

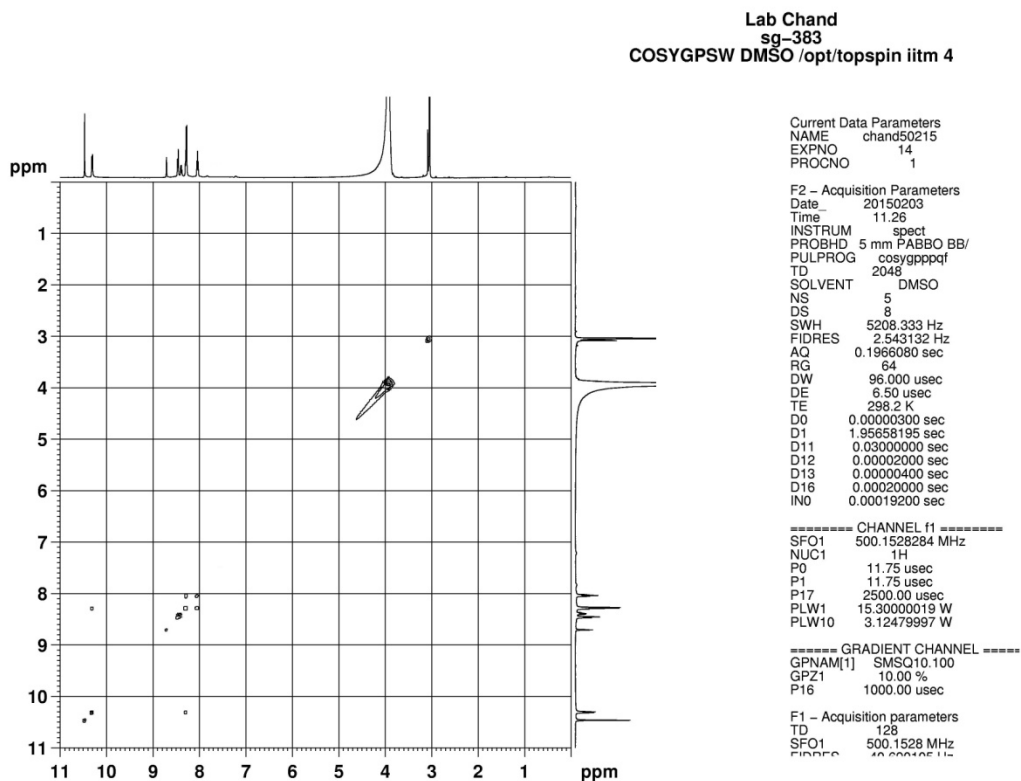


Fig S12: H-H COSY of the complex **2a** in DMSO- d_6 .

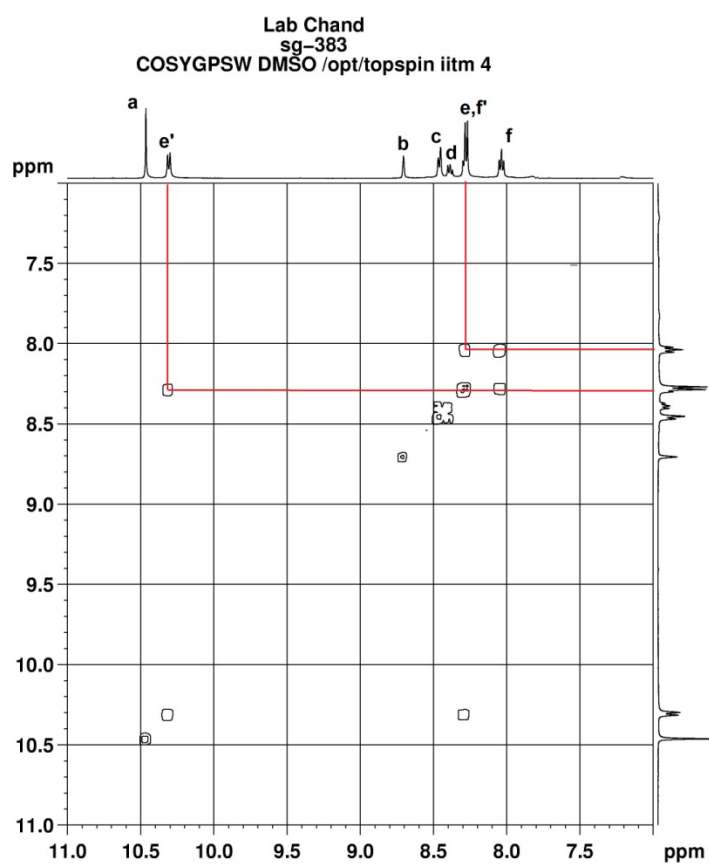


Fig S13: Expansion of H-H COSY of the complex **2a** in DMSO- d_6 .

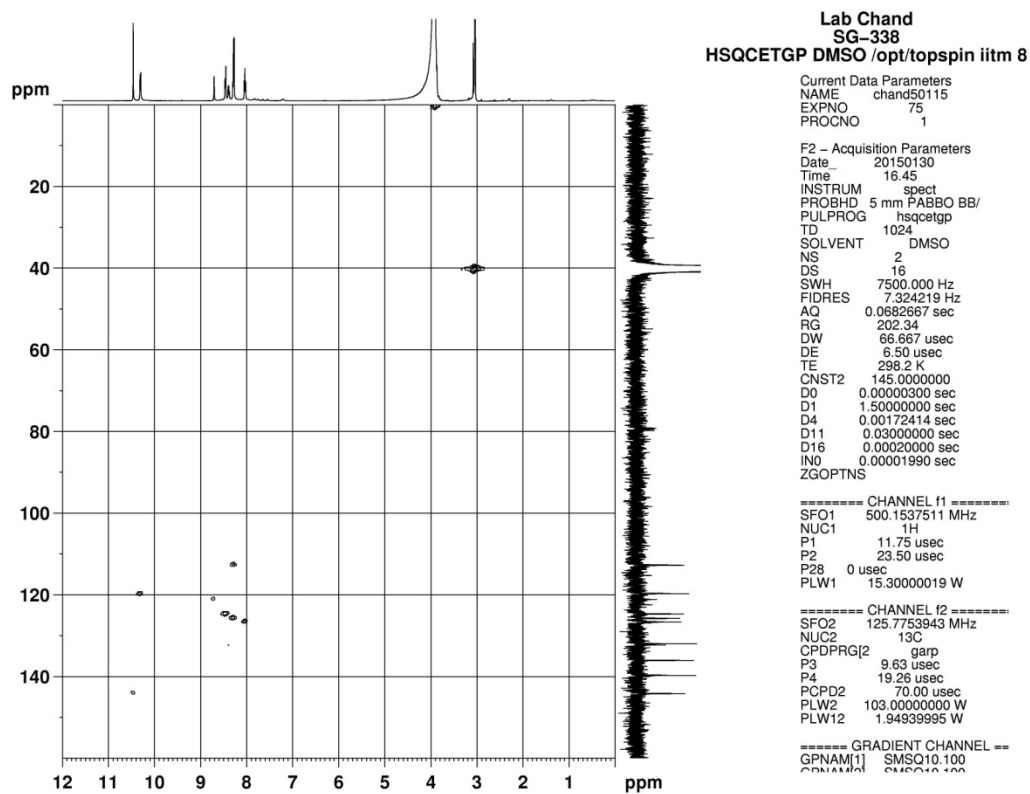


Fig S14: C-H COSY of the complex **2a** in DMSO- d_6 .

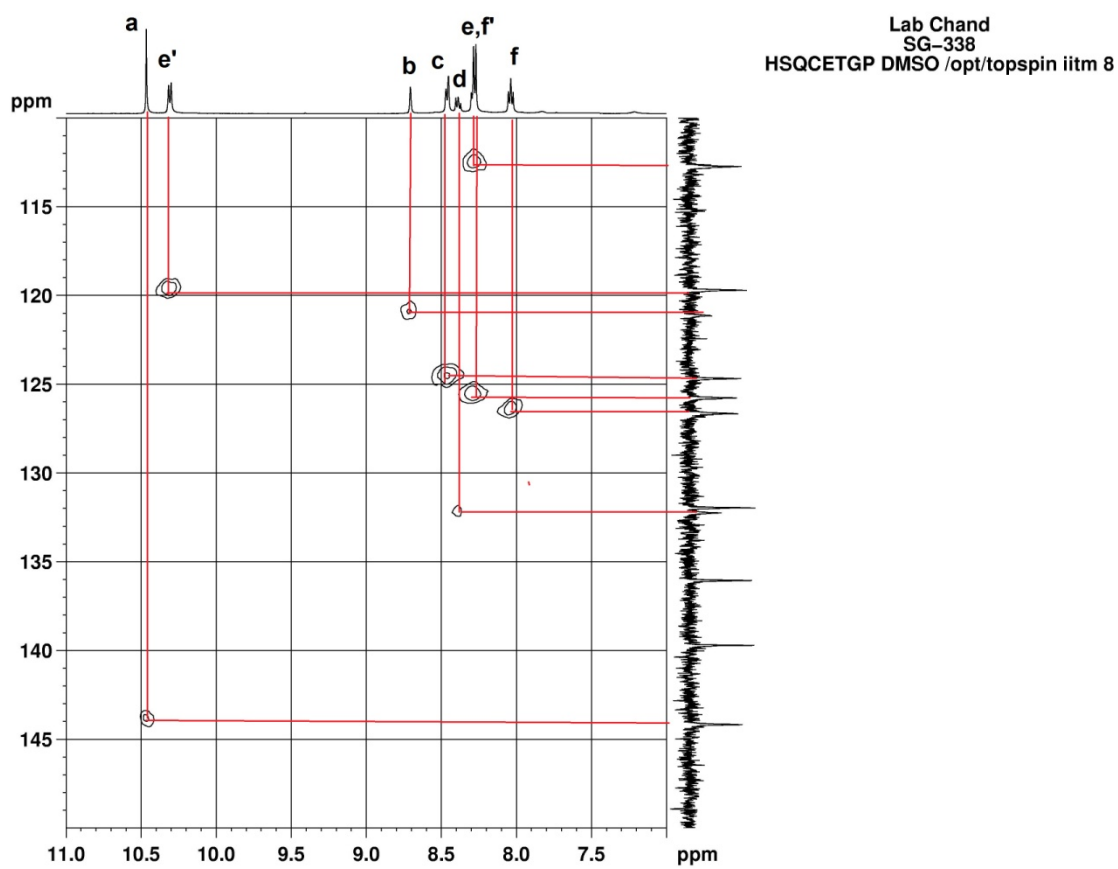
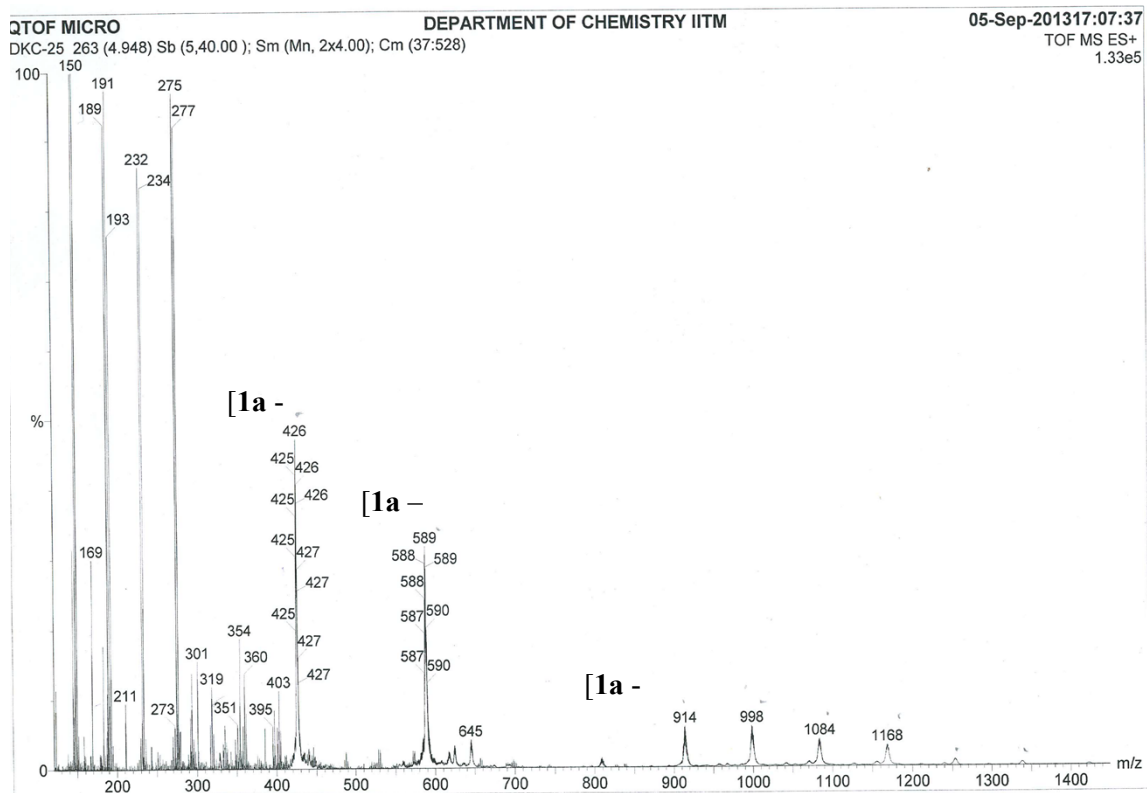


Fig S15: Expansion of C-H COSY of the complex **2a** in DMSO- d_6 .



Fig

S16: ESI-MS of complex 1a.

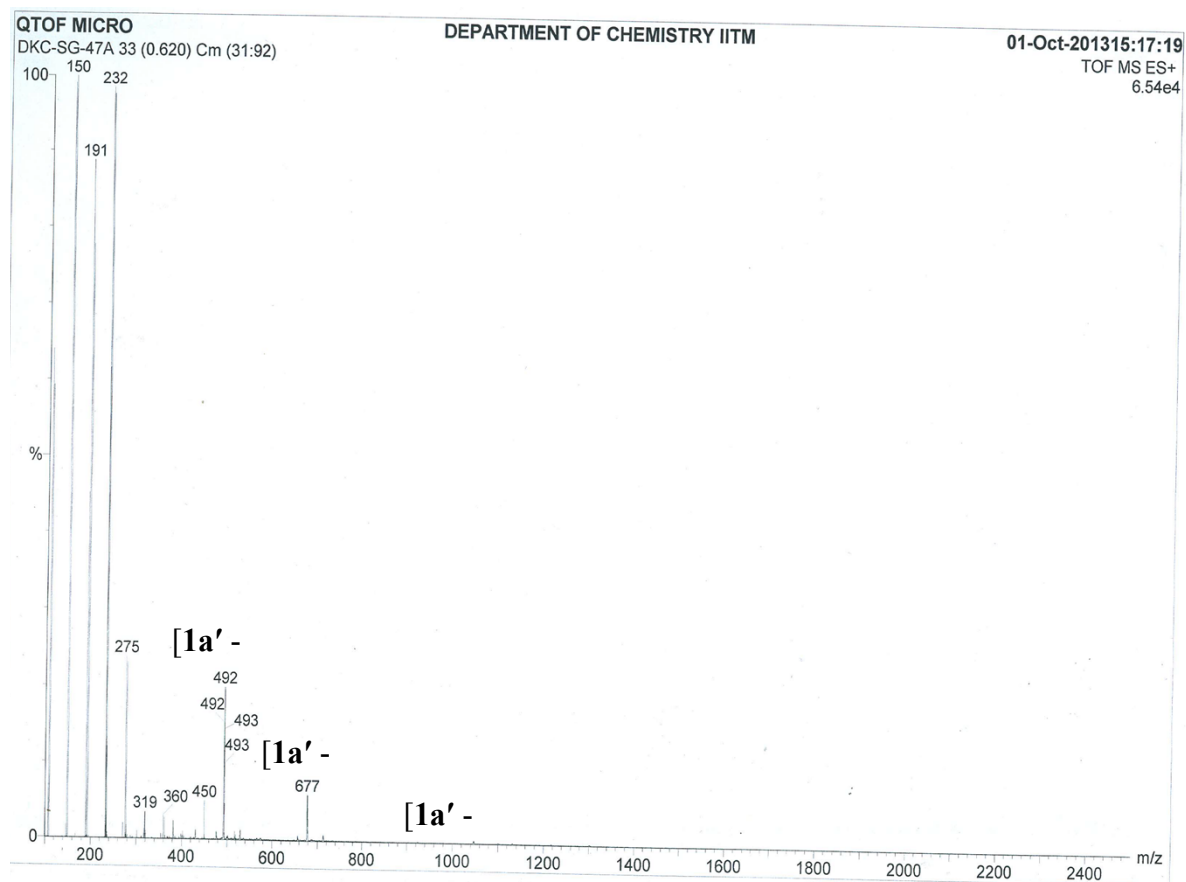


Fig S17: ESI-MS of complex 1a'.

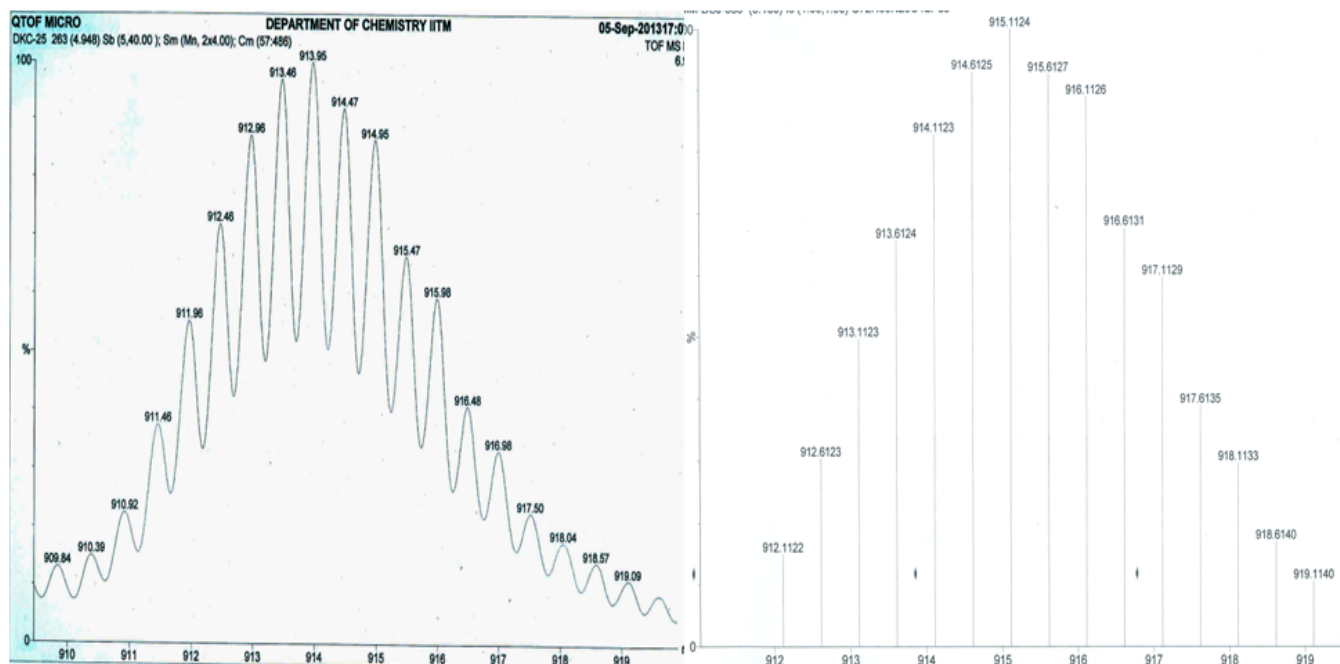


Fig S18: ESI-MS expansion of a) $[1a - 2NO_3]^{2+}$ and b) theoretical pattern.

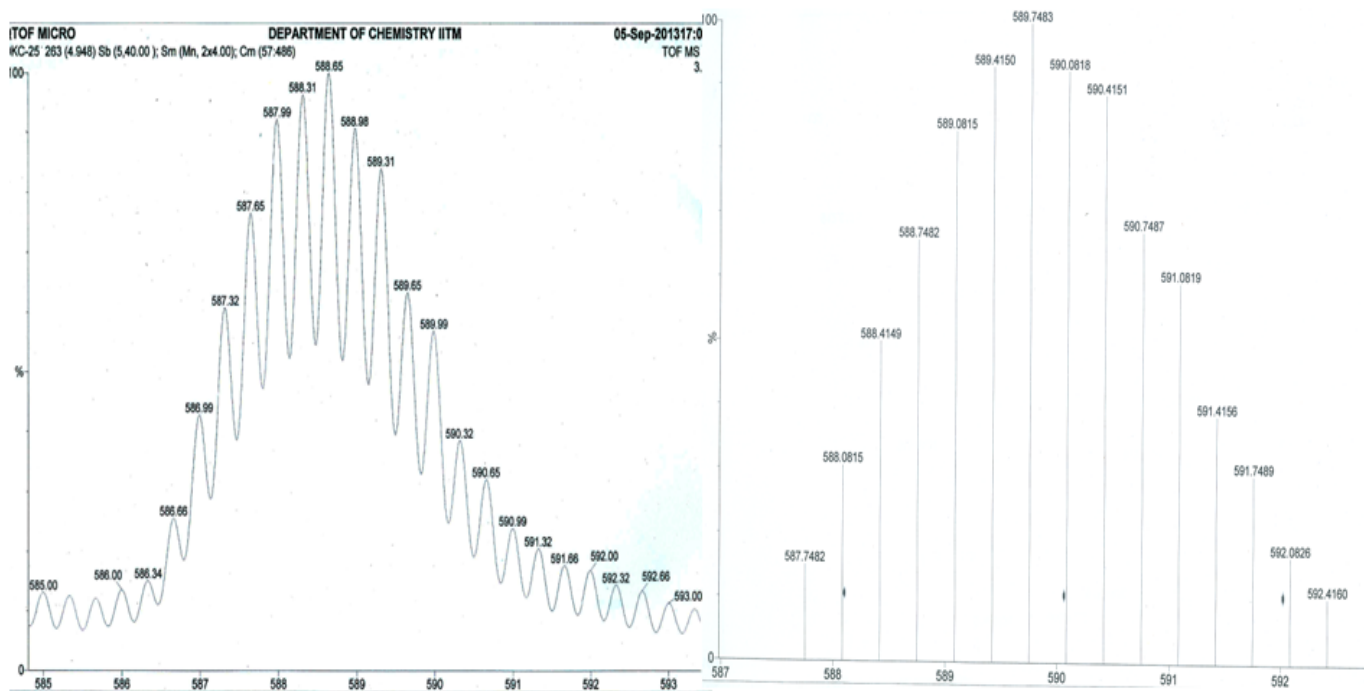


Fig S19: ESI-MS expansion of a) $[1a - 3NO_3]^{3+}$ and b) theoretical pattern.

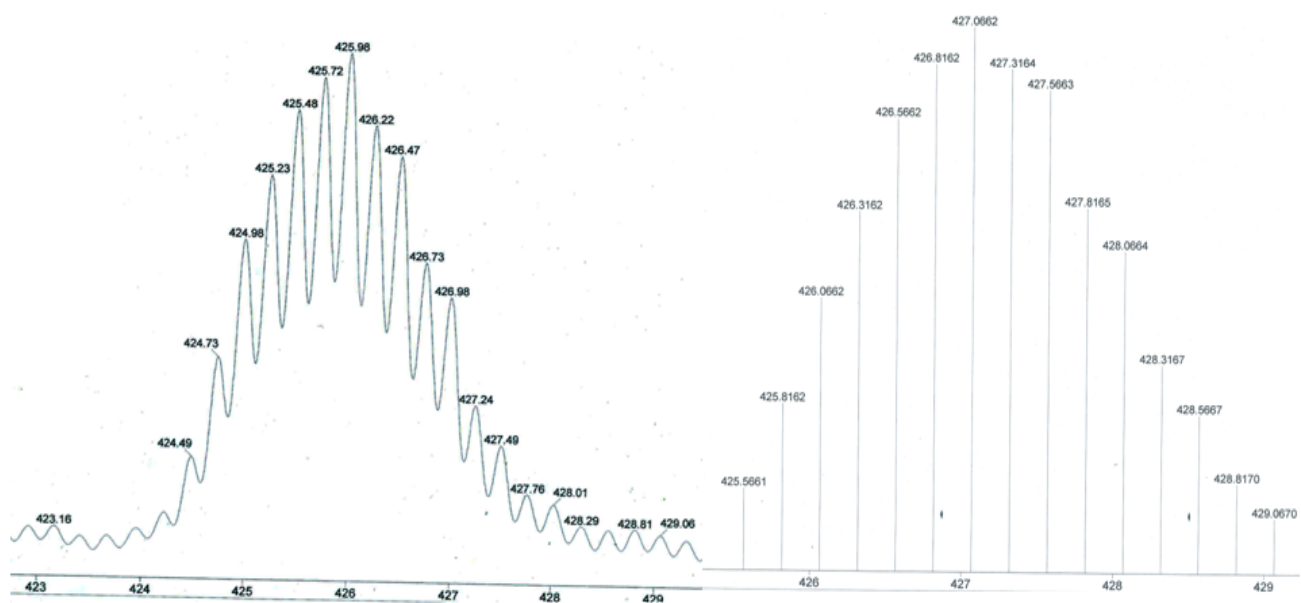


Fig S20: ESI-MS expansion of a) $[1a - 4NO_3]^{4+}$ and b) theoretical pattern.

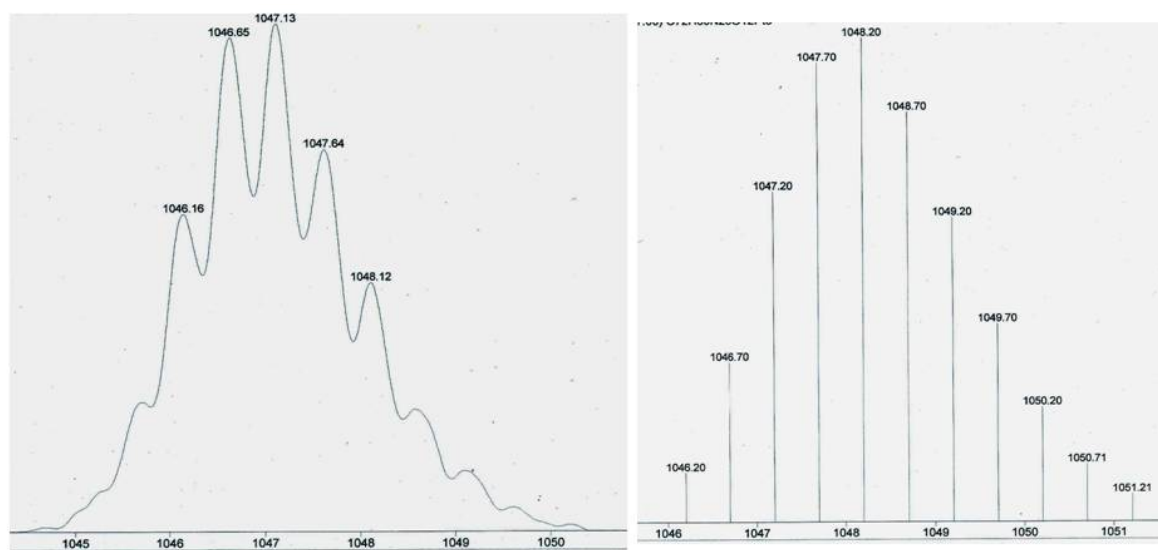


Fig S21: ESI-MS expansion of a) $[1a' - 2NO_3]^{2+}$ and b) theoretical pattern.

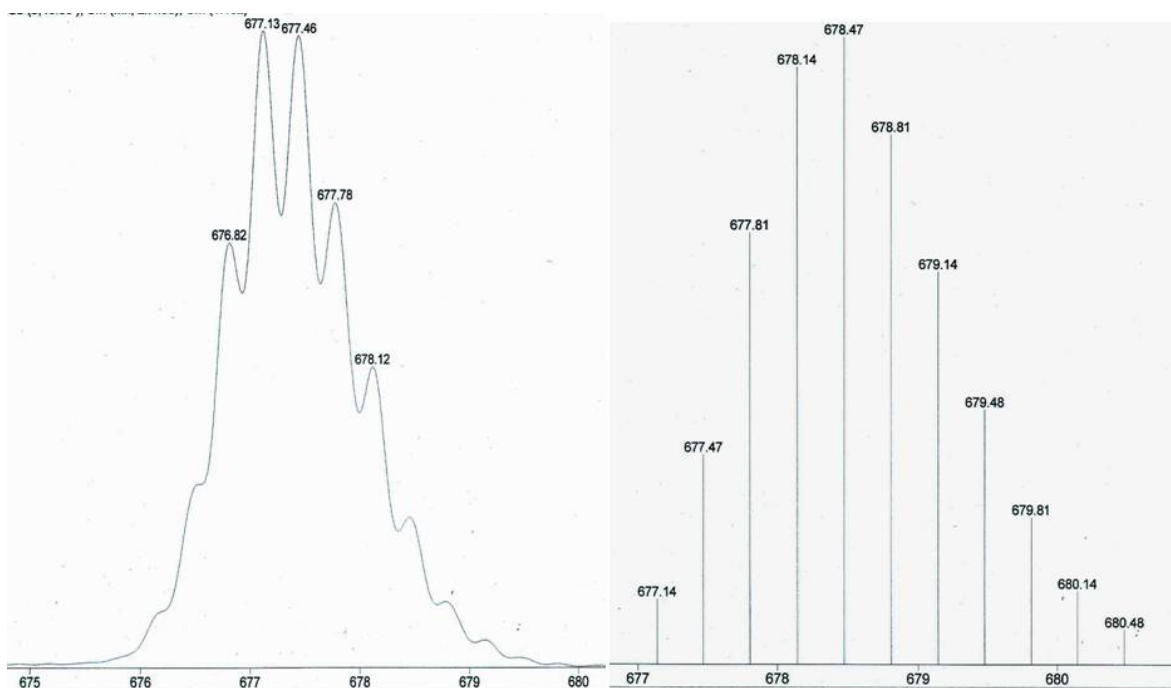


Fig S22: ESI-MS expansion of a) $[1a' - 3NO_3]^{3+}$ and b) theoretical pattern.

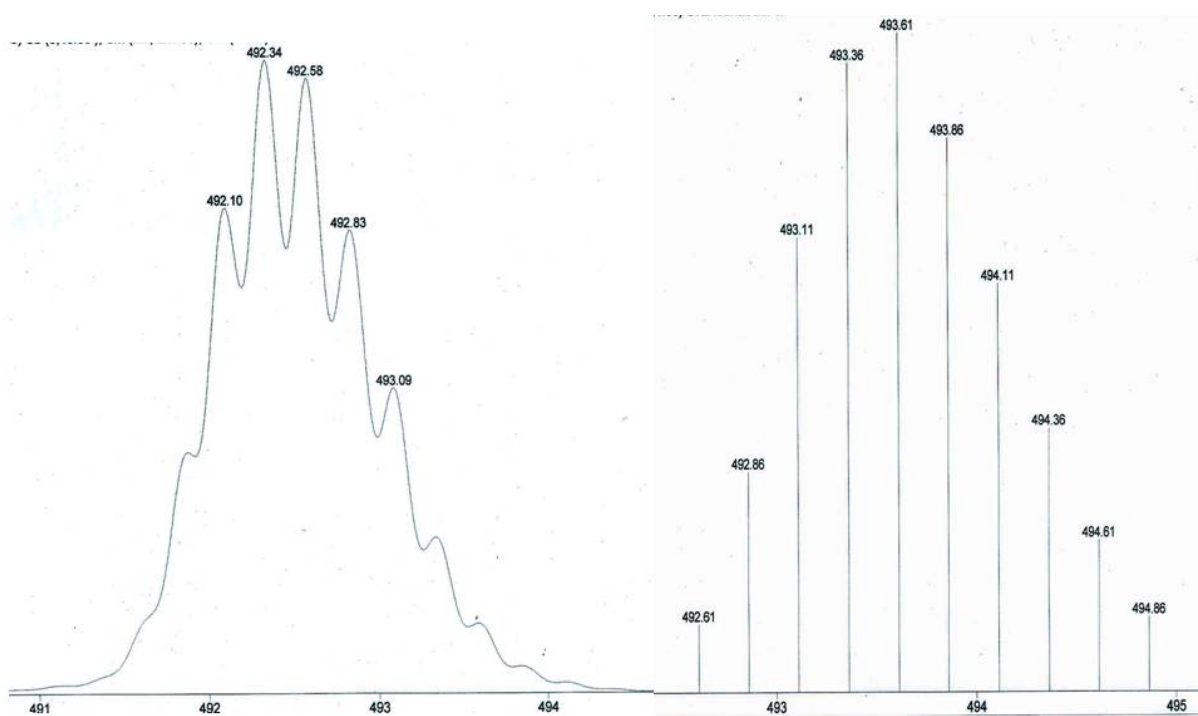


Fig S23: ESI-MS expansion of a) $[1a' - 4NO_3]^{4+}$ and b) theoretical pattern.

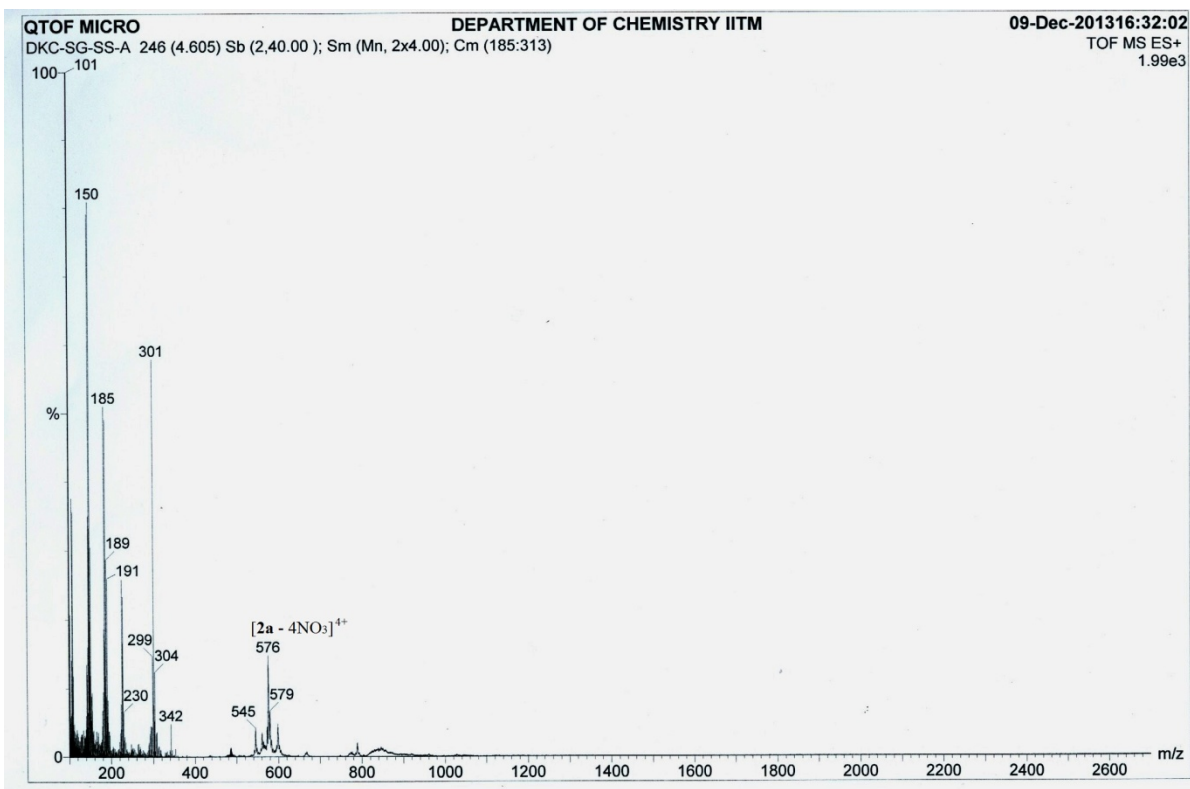


Fig S24: ESI-MS of complex **2a**.

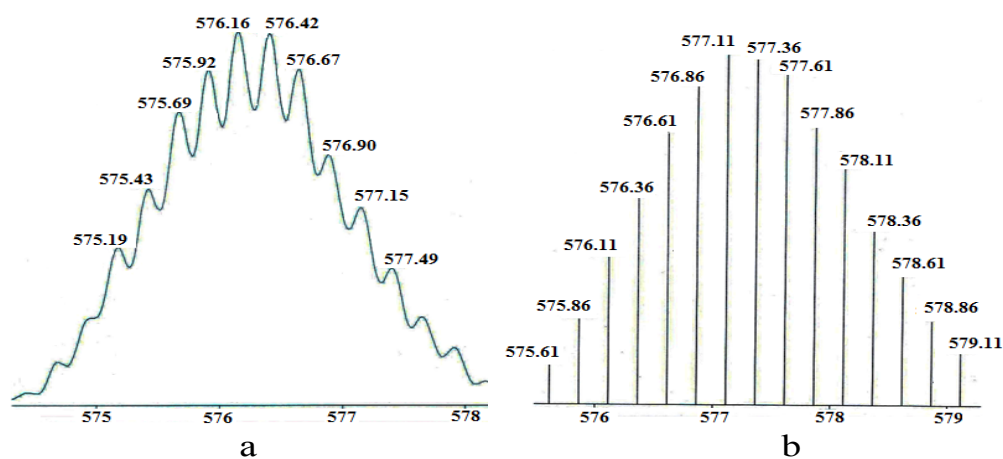


Fig S25: ESI-MS expansion of a) $[2a - (NO_3)_4]^{4+}$ and b) theoretical pattern.

Gelation Test using *in-situ* prepared **2a :** To the PdCl₂ (2 mg, 0.01 mmol) in DMSO (0.5 mL), AgNO₃ (4 mg, 0.22 mmol) was added and the solution was heated for 1 hr at 70 °C. The clear Pd(NO₃)₂ solution was decanted after centrifugation and the ligand, **L2** (7 mg, 0.022 mmol) was added and kept aside for 5-10 min. Opaque gel formation was observed.

Gelation in different solvents: The isolated complex **2a** (20 mg, 0.0078 mmol) was added to 1 mL of solvent/mixture of solvents in clean test tubes as listed below (2% w/v or 20 mM of Pd). The mixtures were shaken vigorously for 10 min at room temperature and kept aside to check the gel formation. (G = Gelation, I = Insoluble.)

Table S1:

S.No	Solvent(s)	Result
1	DMSO	G
2	DMF	G
3	CH ₃ CN : H ₂ O (1:1)	G
4	CH ₃ CN	I
5	CH ₃ OH	I
6	Acetone	I
7	Isopropanol	I
8	Dioxane	I
9	THF	I
10	DCM	I
11	Chloroform	I
12	Hexane	I

(G = Gelation, I = Insoluble.)

Effect of anions on gelation: The ligand, **L2** (7 mg, 0.02 mmol) was added into 0.5 mL of DMSO solution of Pd(X)₂ (0.01 mmol, 20 mM) (X = NO₃⁻, BF₄⁻, ClO₄⁻, OTf, PF₆⁻, OTs⁻ and SbF₆⁻ anions) kept in separate test tubes. The mixtures were shaken vigorously for 10 min at room temperature and kept aside to check the gel formation. (G = Gelation, S = Solution and V = Viscous.)

Table S2:

S.No	Metal anion	Result
1	Pd(NO ₃) ₂	G
2	Pd(BF ₄) ₂	S
3	Pd(ClO ₄) ₂	G
4	Pd(OTf) ₂	G
5	Pd(PF ₆) ₂	S
6	Pd(SbF ₆) ₂	S
7	Pd(OTs) ₂	G
8	Pd(OAc) ₂	V

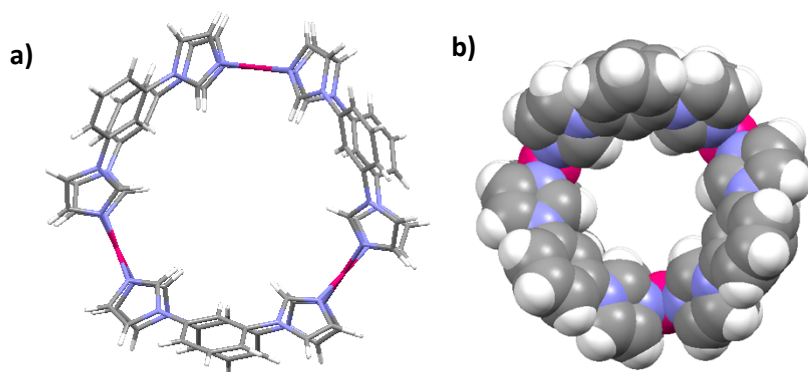


Fig S26: Crystal structure of complex **1a** (crystallized by diffusing acetone to the DMSO solution of the complex) in a) capped stick model b) space filling model showing as a molecular ring. (anions, and cocrystallized solvent molecules are excluded for clarity). (crystal structure of **1a** is reported, see reference 11f of main text, the present crystal structure has a different cell parameters)

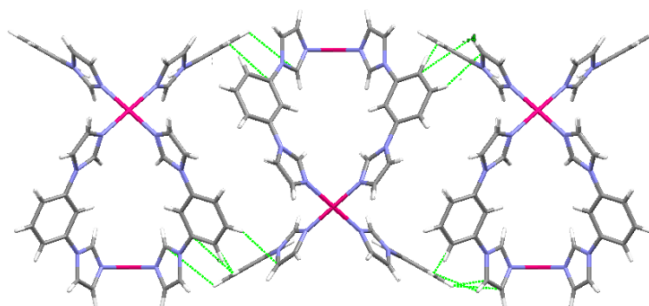


Fig S27: Packing in the crystal structure of **1a** showing intermolecular π - π interactions.

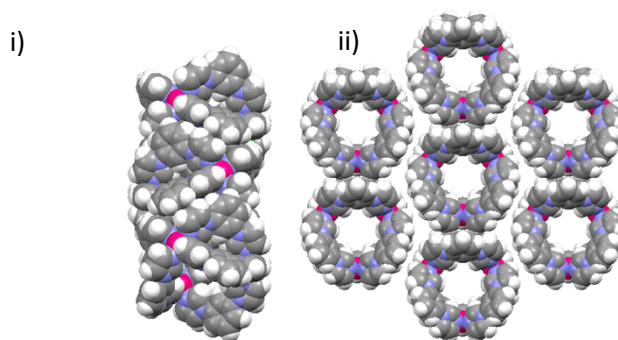


Fig S28 : Channel like arrangement through π - π interactions in the structure of Complex **1a**. View along i) *a* axis and ii) *c* axis.

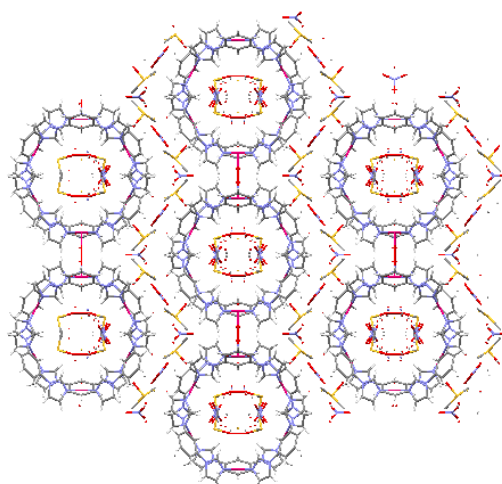


Fig S29: Packing in the crystal structure of the complex **1a**.

Table S3: Summary of X-ray crystallographic data collection and refinement parameters for Complex **1a**. The CCDC number for Complex **1a** is 1024022.

Parameters	Complex 1a
Molecular Formula	$C_{80}H_{84}N_{30}O_{22}Pd_3S_4$
Diffractometer	Bruker Kappa apex2 C
X-ray source	Mo $K\alpha$
λ , Å	0.71073
FW	2265.21
T(K)	296 K
Crystal system	Monoclinic
Space group	$C2/c$
a , Å	37.1846 (11)
b , Å	15.5125 (5)
c , Å	20.9162 (6)
α , deg	90
β , deg	124.221 (1)
γ , deg	90
V , Å ³	9976.2 (5)
Z	4
$F(100)$	4608
No. of reflections measured	43808
Abs. coeff.(mm ⁻¹)	0.70
No. refined parameters	8534
GOF	1.04
$R > 2\sigma$	0.058

Sample preparation for UV-Vis spectroscopy:

A stock solution (1 mM or 1000 μM concentration) was prepared by taking 20 mg of complex **2a**, in 10 mL of DMSO. Then the rest of the solutions were prepared by diluting the stock solution with appropriate volume of DMSO.

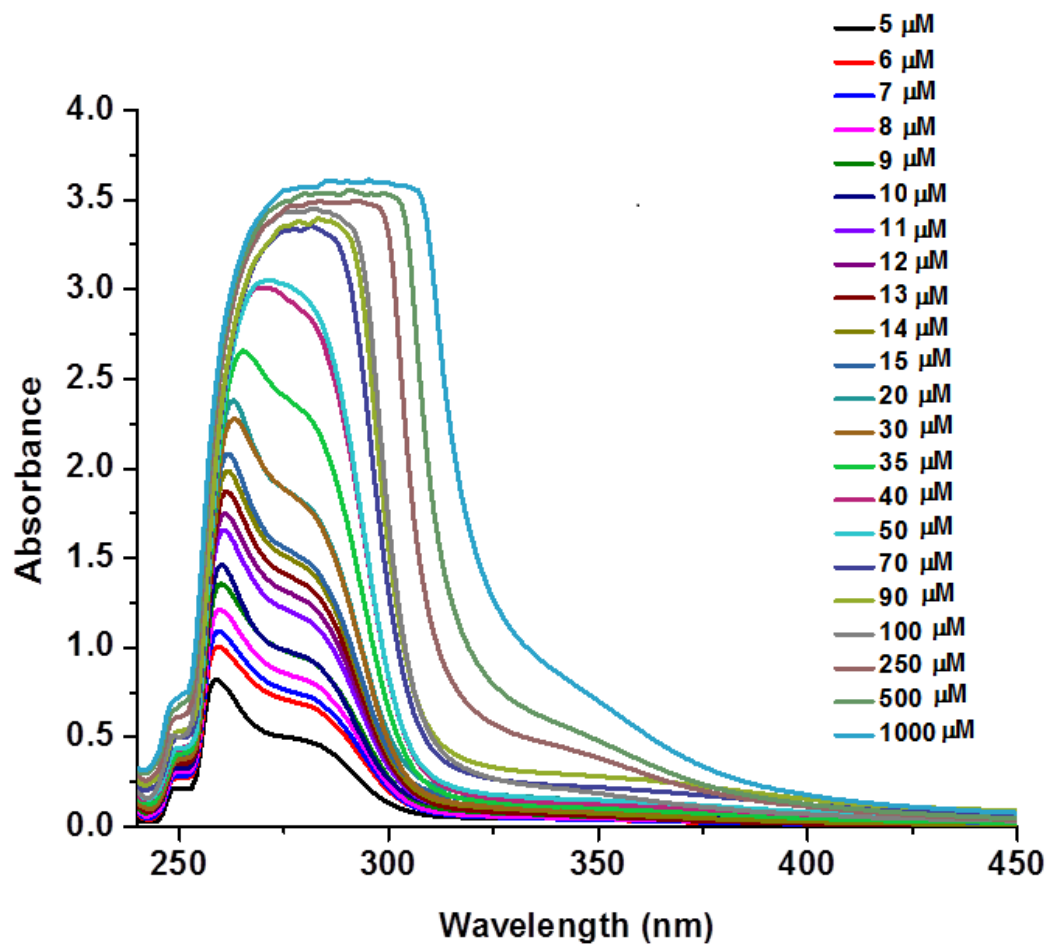


Fig S30: Conc. dependant UV-Vis spectra of the complex **2a** in DMSO solution at room temperature.

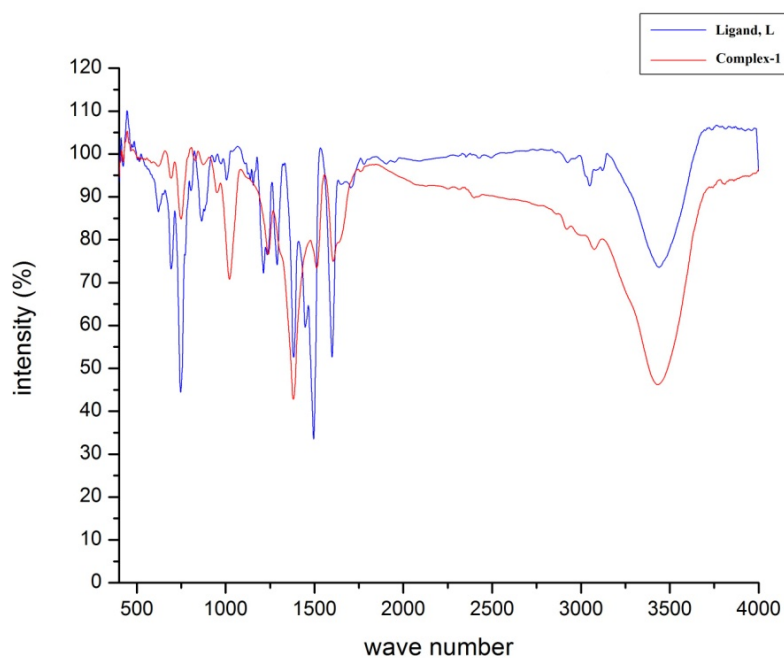


Fig S31: Comparison of FTIR spectra of the xerogel of complex **2a** and the ligand, **L2**

Sample preparation for DLS measurment:

A stock solution (5 mM concentration) was prepared by taking 40 mg of complex **2a**, in 2.5 mL of DMSO. Then 2.5 mM, 1.0 mM and 0.5 mM was prepared by diluting stock solution with appropriate volume of DMSO.

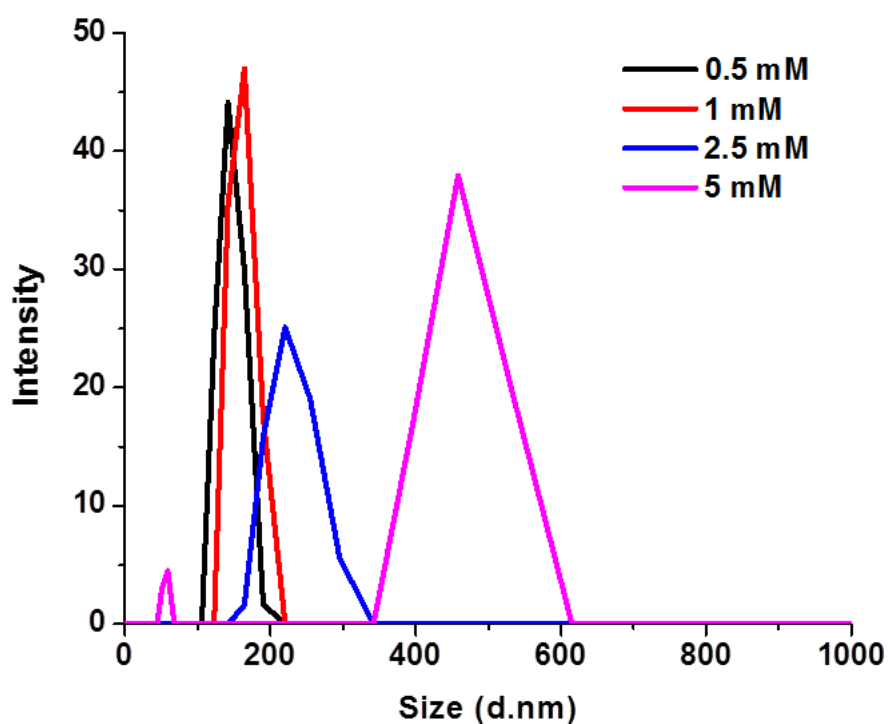


Fig S32: Concentration dependant DLS distributions of the complex **2a** in DMSO solution at room temperature.

Rheology study: For rheology measurements 10 mg of **2a** was dissolved in 0.5 mL of DMSO and stirred for 5 min. Then 0.2 ml of the solution was injected immediately onto a stainless steel plate and allowed to stand for 10 min to afford gel. Then samples were run at a gap of 0.052 mm and 1 Hz oscillation frequency and 0.5% strain.

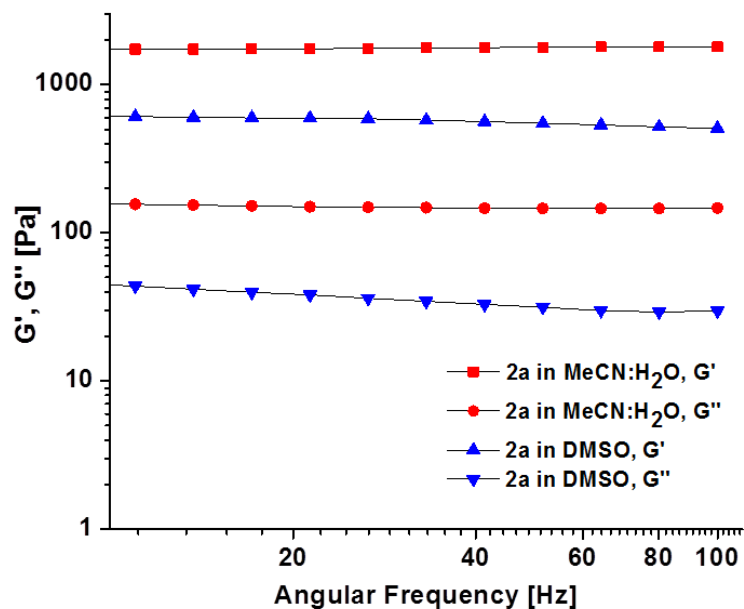


Fig. S33 Frequency dependence of the G' and the G'' of **2a** in DMSO and MeCN:H₂O.

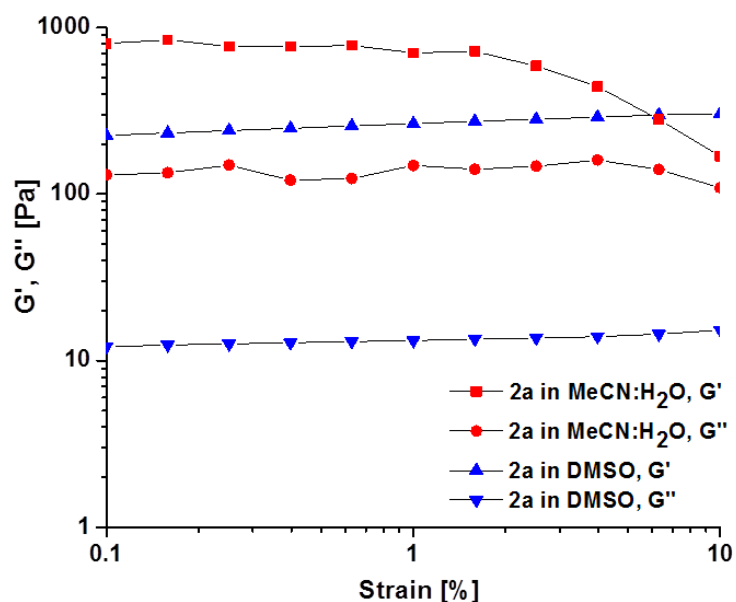


Fig. S34 Strain dependence of the G' and the G'' of **2a** in DMSO and MeCN:H₂O.

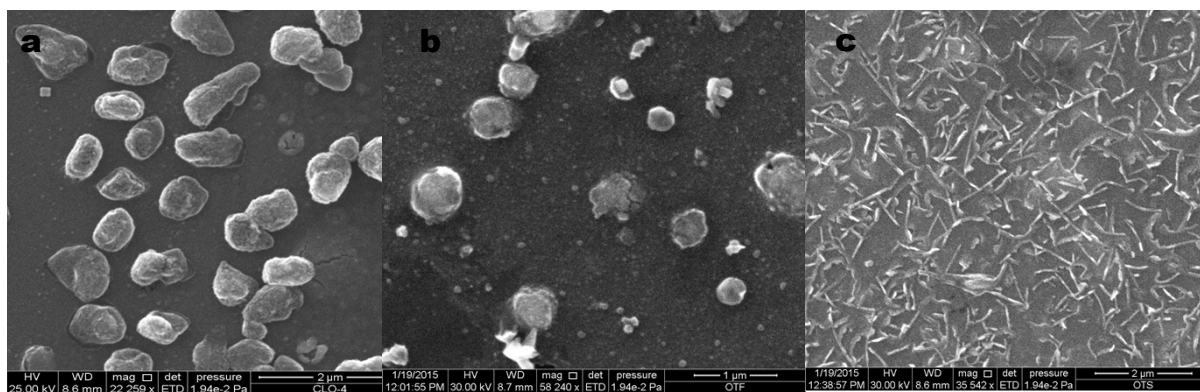


Fig. S35 SEM images of the SMG analogues to **2a** but with other counter anions like: a) perchlorate b) triflate and c) tosylate (2.5 mM in DMSO).

Reversible gel-sol conversion studies

(A) Upon addition of 12 equivalent of tetra-*n*-butylammonium bromide ($\text{Bu}_4\text{N}^+\text{Br}^-$) (15 mg, 0.048 mmol) to the SMG (10 mg of complex **2a**, 0.004 mmol, in 0.5 ml of DMSO-d_6), the gel phase translated into solution phase. It is a known fact that, in the presence of halide ions (X^-), dynamic palladium-nitrogen bond breaks and palladium-halide bond forms. Hence, when halide ions introduced into gel phase, the ligand **L2** got freed as indicated by the conversion of the supramolecular gel to sol phase. This solution phase can transform back to gel phase again by introducing 12 equivalent AgNO_3 (6 mg) into the solution, by reassembly of the trinuclear ring, **2a**.

The gel-sol translation was also seen with the addition of other halides (fluoride, chloride, or iodide) of tetra-*n*-butylammonium ion.

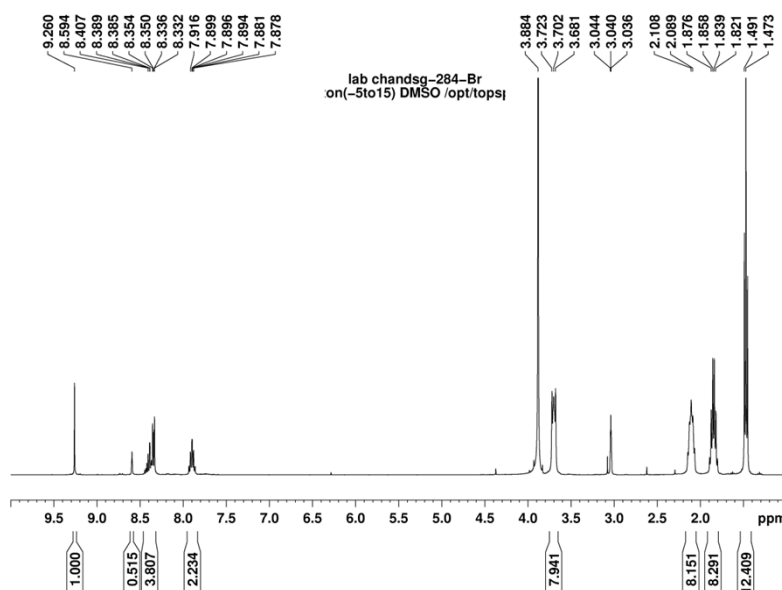


Fig S36: 400 MHz ^1H NMR spectra (in DMSO-d_6) of the ligand, **L2** which got dissociated from the complex **2a** upon addition of $\text{Bu}_4\text{N}^+\text{Br}^-$.

(B) Similarly, gel phase can be tuned to solution phase by adding DMAP (6 mg, 0.048 mmol) to the **SMG**-(10 mg of complex **2a**, 0.004 mmol, in 0.5 ml of DMSO), where upon dis-assembly of the trinuclear ring happens. This gel phase can be restored again by adding few drops of HNO₃, due to the re-assembly of the trinuclear ring, **2a**.

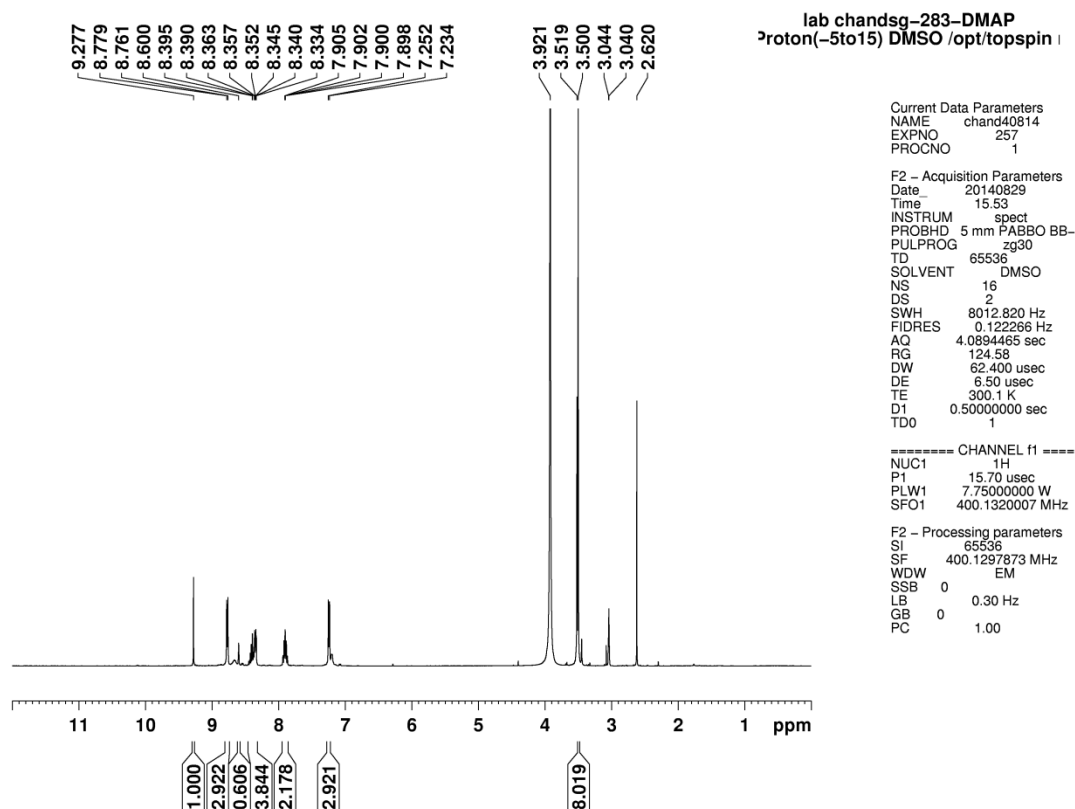


Fig S37: 400 MHz ¹H NMR spectra (in DMSO-d₆) of the ligand, **L2** which comes out from the complex **2a** when DMAP was added.

(C) By adding ethylenediamine (en) (10 μ L 0.02 mmol) into the the **SMG** (20 mg of complex **2a**, 0.008 mmol) in 1 ml of MeCN:H₂O (1:1) system, the en ligand could chelate the Pd(II) ions from the gel of the metal trinuclear ring and forms *bis*(ethylenediamine)Pd(II) complex, which results in the transformation of gel to solution phase and eventually the ligand, **L2** was released from the complex, and appeared as a brown colour precipitate at the bottom of the vial, which is insoluble in the above solvent system. The precipitate was isolated and characterized that confirmed the precipitate as the ligand **L2**. It is noted that, the ligand, **L2** can afford the gel phase again when isolated and combined with a fresh batch of Pd(NO₃)₂ in MeCN-H₂O (1:1) system through reconstruction of the trinuclear ring. [Pd(NO₃)₂ was prepared from PdCl₂ (2 mg, 0.011 mmol), and AgNO₃ (4 mg, 0.022 mmol) in acetonitrile (0.5 mL), and the 0.5 mL of water was added to maintain the ratio of solvents. Then the Pd(NO₃)₂ solution was added to the ligand, **L2**].

By adding en ligand (5 μ L, 0.02 mmol) into the **SMG** (10 mg of complex **2a**, 0.004 mmol) in 0.5 ml of DMSO- d_6 , en ligand could trap the Pd(II) ions from the gel to form *bis*(ethylenediamine)Pd(II) complex, which results in the transformation of gel to solution phase and eventually the ligand, **L2** which could be observed through ^1H NMR technique. However, addition of $\text{Pd}(\text{NO}_3)_2$ to the DMSO solution caused ligand exchange reactions and no gel could be observed.

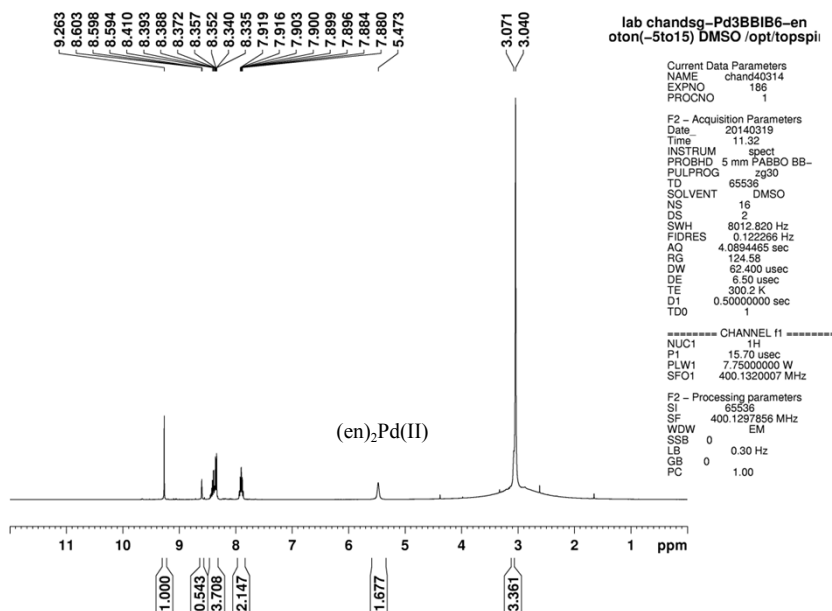


Fig S38: 400 MHz ^1H NMR spectra (in DMSO- d_6) of the ligand, **L2** and $(\text{en})_2\text{Pd}(\text{II})$ which come out from the complex **2a** when en ligand was added.

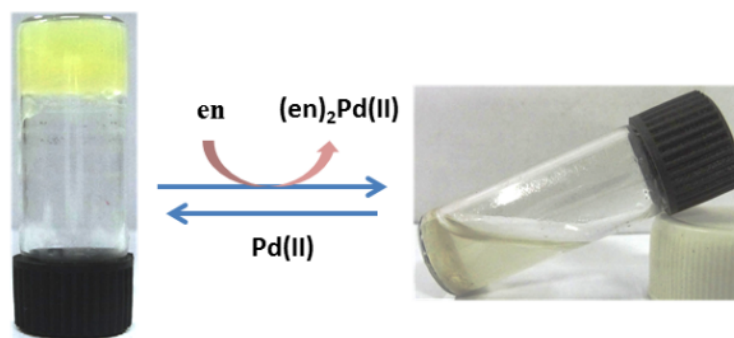


Fig. S39 Schematic representation for the chemical stimuli responsiveness of the SMG by the addition of en and $\text{Pd}(\text{II})$, respectively.

A complex analogous to **2a** but the counter anion is hexafluorophosphate *i.e.* $[\text{Pd}_3(\text{L2})_6](\text{PF}_6)_6$ in DMSO could not give gel. Addition of nitrate anion to this complex, however, assisted the formation of gel as shown below.

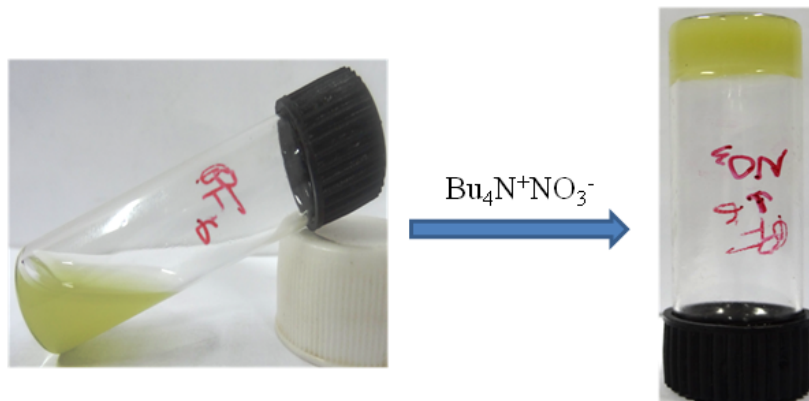


Fig. S40 Conversion of the sol to gel by addition of $\text{Bu}_4\text{N}^+\text{NO}_3^-$ to the DMSO solution of $[\text{Pd}_3(\text{L2})_6](\text{PF}_6)_6$.

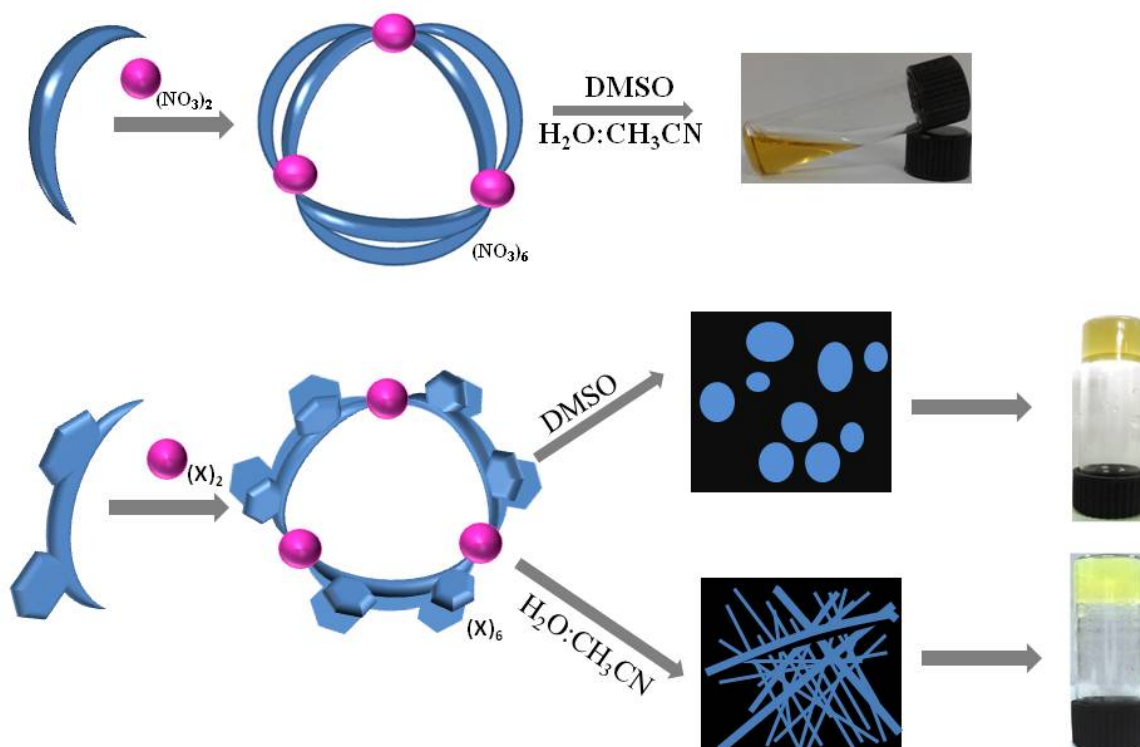


Fig S41 Cartoon representation for the synthesis and gelation study of complex **1a** shown above and complex **2a** shown below. The complex **1a** did not form gel whereas **2a** formed gel. Artistic representation of the SEM diagrams of **2a** as particles and fibres.